Super-resolution Scanning Patch Clamp Reveals Clustering of Functional Ion Channels in Adult Ventricular Myocyte

Anamika Bhargava, Xianming Lin, Pavel Novak, Kinneri Mehta, Yuri Korchev, Mario Delmar,* Julia Gorelik*

Rationale: **Compartmentation of ion channels on the cardiomyocyte surface is important for electric propagation and electromechanical coupling. The specialized T-tubule and costameric structures facilitate spatial coupling of various ion channels and receptors. Existing methods such as immunofluorescence and patch clamp techniques are limited in their ability to localize functional ion channels. As such, a correlation between channel protein location and channel function remains incomplete.**

Objective: **To validate a method that permits routine imaging of the topography of a live cardiomyocyte and study clustering of functional ion channels from a specific microdomain.**

Methods and Results: **We used scanning ion conductance microscopy and conventional cell-attached patch clamp with a software modification that allows controlled increase of pipette tip diameter. The sharp nanopipette used for topography scan was modified into a larger patch pipette that could be positioned with nanoscale precision to a specific site of interest (crest, groove, or T-tubules of cardiomyocytes) and sealed to the membrane for cell-attached recording of ion channels. Using this method, we significantly increased the probability of detecting activity of L-type calcium channels in the T-tubules of ventricular cardiomyocytes. We also demonstrated that active sodium channels do not distribute homogenously on the sarcolemma instead, they segregate into clusters of various densities, most crowded in the crest region, that are surrounded by areas virtually free of functional sodium channels.**

Conclusions: **Our new method substantially increases the throughput of recording location-specific functional ion channels on the cardiomyocyte sarcolemma, thereby allowing characterization of ion channels in relation to the microdomain where they reside. (*Circ Res*. 2013;112:1112-1120.)**

Key Words: calcium channels ■ cardiomyocyte ■ cardiomyocyte structure ■ electrophysiology ■ ion channel ■ scanning ion conductance microscopy ■ sodium channels

The sarcolemma of adult cardiomyocytes includes numerous heterogeneous signaling microdomains where several types of ion channels, receptors, and cytoskeletal elements coexist.[1–3] The clustering of these macromolecular complexes is essential to the proper timing of molecular events that couple electric activation with the contraction of the cardiomyocyte.[4] L-type calcium channels (LTCCs), for example, are functionally and spatially coupled to the sarcoplasmic reticulum calcium release channel;[4,5] lack of synchronization of calcium influx through LTCCs can contribute to contractile dysfunction in myocardial hypertrophy and heart failure.[6] There is evidence that the ultrastructural integrity of the dyad is critical to proper electric and mechanical function.[5] Sodium channel proteins also segregate into defined subdomains. In particular, recent data show that $Na_V1.5$ distributes into 2 separate pools with distinct functional properties, one at the intercalated disc, where $Na_V1.5$ interacts with ankyrin-G, synapse-associated protein 97, and plakophilin 2, and a different one, where $Na_V1.5$ associates with the syntrophin–dystrophin complex.[7–9] For the most part, the findings described were obtained by immunofluorescence

In This Issue, see p 1085
Editorial, see p 1088

Original received November 1, 2012; revision received February 25, 2013; accepted February 25, 2013. In January 2013, the average time from submission to first decision for all original research papers submitted to *Circulation Research* was 12.2 days.

From the Department of Cardiovascular Sciences (A.B., J.G.) and Department of Medicine (P.N., Y.K.), National Heart and Lung Institute, Imperial College, London, United Kingdom; and The Leon H Charney Division of Cardiology, New York University School of Medicine, New York, NY (X.L., K.M., M.D.).

*These authors contributed equally.

The online-only Data Supplement is available with this article at http://circres.ahajournals.org/lookup/suppl/doi:10.1161/CIRCRESAHA.111.300445/-/DC1.

Correspondence to Julia Gorelik, Imperial College London/National Heart and Lung Institute, 4th floor, Imperial Centre for Translational and Experimental Medicine (ICTEM), Hammersmith Campus, Du Cane Road, London W12 0NN, E-mail j.gorelik@imperial.ac.uk, or to Mario Delmar, The Leon H Charney Division of Cardiology, New York University School of Medicine, New York, NY. E-mail Mario.Delmar@nyumc.org

Nonstandard Abbreviations and Acronyms	
ID	internal diameter
LTCC	L-type calcium channel
SICM	scanning ion conductance microscopy

microscopy methods. Unfortunately, immunofluorescence microscopy only localizes the position of channel proteins grossly within a subcellular domain, but it does not establish the extent to which those proteins form functional channels. As such, a correlation between channel protein location and ion channel function remains incomplete.

The current study reports a technical advancement that permits routine imaging of the topography of a live cell and then recording of ion channels from a selected site with nanoscale precision. The new procedure has a throughput similar to that of conventional cell-attached patch clamp with the advantage of substantially higher spatial resolution. Using this system, we have characterized for the first time the clustering of functional sodium and calcium channels in the cardiomyocyte sarcolemma. The method, heretofore called super-resolution scanning patch clamp for its conceptual analogy to optical methods that enhance the resolution of an imaging system into the nanoscale (super-resolution microscopy),[10] uses the platform of scanning ion conductance microscopy (SICM)[11] combined with conventional cell-attached patch clamp. Previous attempts to combine both methods were limited by the conflicting needs of a fine-tipped pipette (≤100 nm internal diameter [ID]) that permits scanning at high spatial resolution and a pipette with larger diameter to increase the probability of capturing functional ion channels under the patch. Here, we validate a new method that uses the computer-controlled movements of piezo-actuators to progressively clip the tip of the pipette to achieve a desired tip diameter. Following this approach, the fine-tipped pipette (≈100 nm ID) used for the topography scan is modified into a patch pipette with a preselected larger tip diameter (≈300 nm ID) that can be moved back to a precise coordinate, centered at a site of known topology, and then sealed to the membrane for recording of functional ion channels. Using this method, we confirm that LTCCs are prominently clustered in the T-tubule region of adult cardiomyocytes. We also demonstrate for the first time that sodium channels in the midsection of cardiomyocytes (ie, away from the intercalated disc)[7] are not homogeneously distributed along the surface. Instead, they form clusters of various densities that are surrounded by areas free of functional sodium channels. We further show that the crest region of the sarcomere contains the clusters of largest density and has the highest likelihood of finding zero channels in a patch. Overall, this method surpasses detection of ion channel proteins by immunofluorescence microscopy in terms of spatial resolution, concurrent identification of extracellular structures, and selective, highly quantitative identification of the protein population that forms functional channels. The potential of this method in providing novel quantitative parameters in the study of cellular/molecular electrophysiology is discussed.

Methods

Cardiomyocyte Isolation and Cell Plating

All animal procedures related to LTCC studies conformed to the UK Animals (Scientific Procedures) Act 1986 for rat cardiomyocytes isolation. Studies of sodium channel properties were performed in accordance with New York University guidelines for animal use and care (Institutional Animal Care and Use Committee Protocol 101101–02 to M.D.) and conformed to the *Guide for the Care and Use of Laboratory Animals* (published by the US National Institutes of Health Publication 58-23, revised 1996). Cardiomyocytes from adult rats were isolated by the Langendorff perfusion method as described.[12] Adult mouse ventricular myocytes were obtained by enzymatic dissociation following standard procedures. Briefly, mice were injected with 0.1 mL heparin (500 IU/mL intraperitoneally) 20 minutes before heart excision and anesthetized by carbon dioxide inhalation. Deep anesthesia was confirmed by lack of response to otherwise painful stimuli. Hearts were quickly removed from the chest and placed in a Langendorff column. The isolated hearts were then perfused sequentially with low calcium and an enzyme (collagenase; Worthington) solution. Ventricles were cut into small pieces and gently minced with a Pasteur pipette. Calcium concentration was then increased gradually to normal values. After isolation, cardiomyocytes were plated on laminin-coated coverslips or dishes and left to adhere for at least 30 minutes before the start of experiments. Cardiomyocytes were used on the same day of isolation. Cells were washed once with the external recording solution and mounted on the microscope stage for recordings.

Instrumentation for Super-resolution Scanning Patch Clamp

SICM

SICM is a noncontact scanning probe microscopy technique based on the principle that the flow of ions through the tip of a nanopipette filled with electrolytes decreases when the pipette approaches the surface of the sample.[11,13,14] The result is a 3-dimensional topography image of live cells with resolution of up to ≤20 nm.[15] All topographical images in this study were recorded using a variant of SICM called hopping probe ion conductance microscopy,[16] implemented on a software platform that controls the ICnano sample scan system[13] (Ionscope). The scan head of the ICnano system consists of a 3-axis piezo-translation system (Physik Instrumente, United Kingdom) with a 100 × 100-µm *x*–*y* piezo-stage for sample positioning and 38-µm *z* axis piezo-actuator for the vertical movement of the pipette mounted on the stage of a conventional inverted microscope (Diaphot 200; Nikon). Schematic of the set-up is presented in Figure 1. Glass nanopipettes of ≈100 nm ID pulled from 1.0 mm outer diameter, 0.5 mm ID borosilicate capillary were used in all experiments. Axopatch 200A/B patch-clamp amplifiers (Molecular Devices) were used to measure the pipette current as well as to record ion channel activity. Cell-attached currents were digitized using Digidata 1200B and a pClamp 10 data acquisition system (Axon Instruments; Molecular Devices).

Controlled Modification of the Pipette Diameter

The tip of the pipette was clipped using a software-controlled movement of the piezo-actuator. Details of the development of this method are under consideration for publication in *Neuron*. Briefly, after generating the topographical image of the cardiomyocyte surface, the pipette (≈100 nm ID) was moved to an area clear of cells or debris. At that coordinate, the rate at which the pipette approached the sample during scanning was increased to ≈500 nm/ms, and the duration of the excursion (from fall to rise) was adjusted to 500 ms. This maneuver caused the pipette tip to clip against the solid bottom of the dish (Figure 2A and 2B). The pipette resistance was continuously monitored and the clipping motion was stopped once the current through the pipette reached the desired level. At that point, the pipette was repositioned to spatial coordinates that were selected based on the topography image recorded with the sharp pipette (Figure 2C).

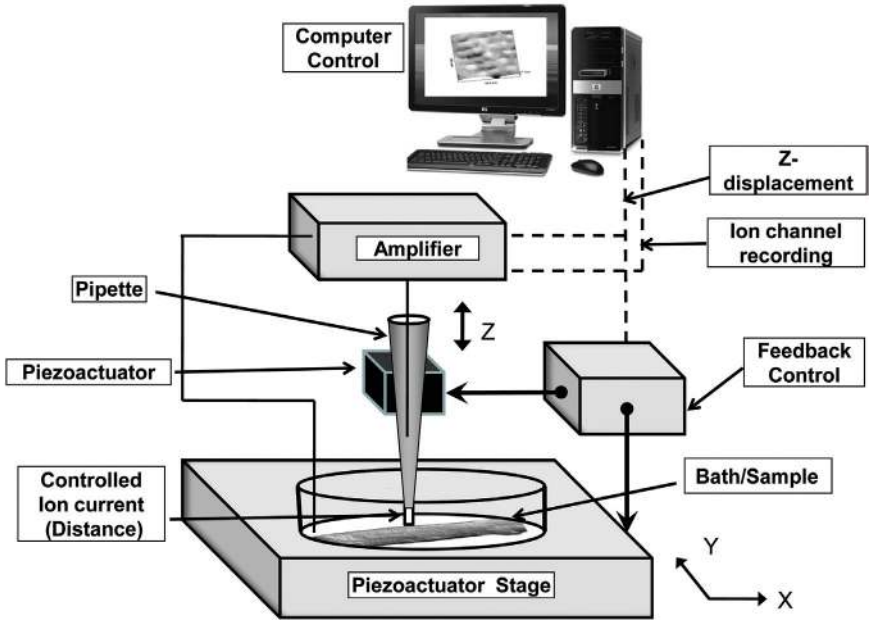

Figure 1. Set-up for super-resolution scanning patch clamp. The scanning/patch pipette is mounted on a piezo-translation platform and connected to a patch-clamp amplifier. The amplifier's output drives a feedback control amplifier to control the pipette's piezo, which provides a Z-only directional movement (**top** and **bottom**). It also provides a drive to the nanopositioning piezo-actuator stage (**bottom**) raster scanning in 2 directions (X Y). Computer-controlled software provides a user interface to control the set-up. Sample is placed on the stage without any fixation or additional preparation.

The lateral error of repositioning was determined by the *x–y* piezo-actuators (PI-621.2CD; Physik Instrumente). The resolution of the PI-621.2CD *x–y* piezo-stage in the closed loop operation is 0.4 nm and the repeatability (error between repeated returns to the same point) is ±2 nm (complete set of specifications in http://www.physikinstrumente.com/en/pdf/P620_2_Datasheet.pdf). Of note, tip size is only a determinant of the lateral resolution of a scan[17] and it does not affect repositioning. Once the *x, y* coordinates of the structure are established, the precision with which the pipette is returned to a specific location is determined exclusively by the resolution and repeatability of the *x–y* piezo-actuators. As such, though the recording pipette occupies a larger area after clipping, its center is repositioned with an accuracy of ±2 nm.

Image Recording Stability

Additional experiments confirmed that the repositioning error was below the resolution limit of SICM. The results are shown in Online Figure I. A specific area of an adult ventricular myocyte was scanned twice (scan 1 and scan 2) with ≈100 nm ID pipette (spatial resolution 50 nm). The 2 scans were pseudocolored in red and green, respectively. The images were then superimposed, yielding a yellow pixel at those locations where red and green were in the registry. Notice that the 2 images were virtually identical (all pixels in yellow), with no apparent offsets. These results indicate that our spatial error at repositioning was less than the overall spatial resolution of the recording system.

Definition of Recording Sites

Figure 3 illustrates the recording positions described in this article. Figure 3A shows an image of a cardiomyocyte and the pipette, as seen optically. Figure 3B shows the 3 possible recording locations defined by the SICM-based topology map: T-tubule; crest; and Z-grooves. A depth profile along the *x–y* plane marked by the black dotted line is shown on the right side. The profile reveals the periodic crests and grooves characteristic of adult cardiac myocytes. The Z-grooves correspond to the position of the Z-lines in the intracellular side.[18] The distance between crests (or Z-grooves) is ≈2 μm and the recording probe travels into the T-tubule to a depth of ≈100 to 300 nm (see vertical scale). As illustrated in Figure 3C and 3D, this configuration allowed detection of ion channels (Figure 3C) or the lack thereof (Figure 3D) in relation to the precise location of recording. The cell-attached configuration was formed within 5 to 6 minutes after the SICM image was recorded. Based on estimates correlating pipette resistance to pipette tip diameter,[19] we calculated that clipping the tip increased the pipette ID ≈3-fold, from 100 nm to 300 nm. Assuming a hemispherical shape of the

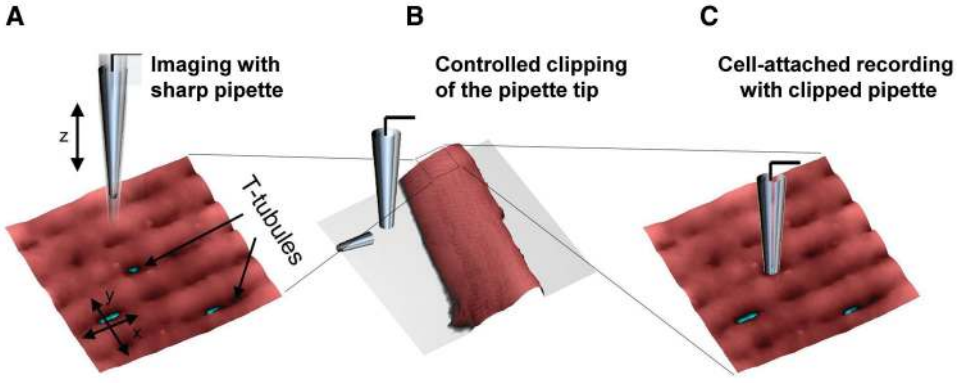

Figure 2. Pipette clipping procedure. A, A sharp high-resistance pipette is used to resolve the topographical structure of the cardiomyocyte. **B**, The pipette is moved to a cell-free area on the dish and the fall rate is increased (as described in the text) to clip the pipette tip. **C**, The pipette is then returned to the structure of choice and patch clamp can be performed with a pipette of wider tip than (**A**).

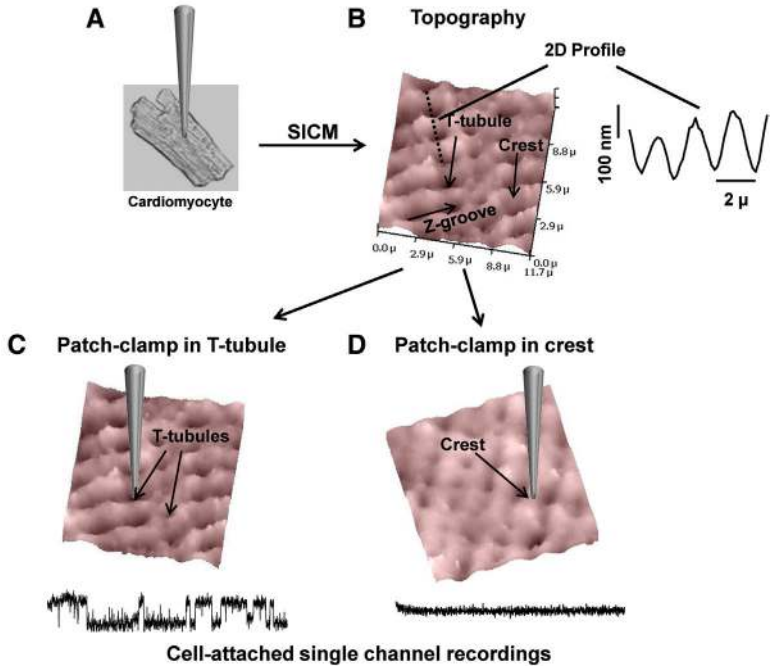

Figure 3. Schematic of super-resolution scanning patch clamp. **A**, A single rat cardiomyocyte and pipette as seen optically. **B**, A 10 µm×10 µm scan of a cardiomyocyte revealing topographical structures such as the Z-groove, T-tubule, and crest. A depth profile along the *x–y* plane marked by the black dotted line is shown on the right side. Super-resolution scanning patch clamp of T-tubule (**C**) and crest (**D**) allowed for detection (or lack thereof) of functional ion channels. The traces below represent L-type calcium channels activity that is usually seen in T-tubules of cardiomyocytes as opposed to crest. SICM indicates scanning ion conductance microscopy.

membrane patch, this increase in pipette diameter corresponds to a 10-fold increase in the area under the patch pipette, thus increasing the probability of capturing a channel (or channel cluster) under the patch.

Electrophysiological Recordings

After repositioning the pipette, the noncontact mode of SICM was turned off and the pipette was lowered using the piezo-actuator until it touched the membrane (indicated by an increase in the pipette resistance); as in conventional patch clamp, slight suction sealed the cell membrane to the glass pipette. All electrophysiological recordings were obtained using the cell-attached patch clamp configuration and were only included if seal resistance was larger than 5GΩ and if leak current at 0 mV remained constant at 0 pA.

For recording of LTCCs, cardiomyocytes were bathed in an external solution containing the following (in mmol/L): 120 K-gluconate, 25 KCl, 2 $MgCl_2$, 1 $CaCl_2$, 2 EGTA, 10 glucose, 10 HEPES, pH 7.4 with NaOH, and ≈290 mOsm. Pipettes were filled with an internal recording solution containing the following (in mmol/L): 90 $BaCl_2$, 10 HEPES, 10 sucrose, pH 7.4 with TEA-OH, and ≈250 mOsm. The membrane under the patch was held at a voltage of −80 mV and voltage pulses were applied from −30 to +30 mV in incremental steps of 10 mV. To determine the effect of isoproterenol on the open probability of LTCCs, repetitive depolarizing steps of 1 second duration to +10 mV were applied from a holding potential of −80 mV at an interpulse interval of 2 seconds. Open probability was calculated from at least 15 to 20 consecutive sweeps before and after 5 minutes of perfusion of 10 µmol/L isoproterenol. Data were recorded at a sampling rate of 10 kHz and filtered at 2 kHz. The applied voltage was corrected for a liquid junction potential of −16.7 mV. For recording of sodium currents, pipettes were filled with a solution containing the following (in mmol/L): NaCl 148, NaH_2PO_4 0.4, $MgCl_2$ 1, $CdCl_2$ 0.2, KCl 5.4, HEPES 15, $CaCl_2$ 1.0, and glucose 5.5, pH 7.4 with NaOH. When indicated, tetrodotoxin 30 µmol/L was added to the internal pipette solution. Cells were maintained in a solution containing the following (in mmol/L): 0.33 NaH_2PO_4, 5 HEPES, 1.0 $CaCl_2$, and 140 KCl, pH 7.4 with KOH, thus depolarizing the membrane potential to a value estimated to be near zero. To assess the presence of fast inward currents, the membrane under the patch was held at −120 mV and voltage clamp pulses of 500 ms were applied every 3 seconds to −30 mV. To define the unitary current–voltage relation, 500 ms voltage clamp pulses were applied to −80, −70, −60, and −50 mV from a constant holding potential of −120 mV.

Data Analysis

Single-channel data were analyzed using Clampex version 10.0. All graphs and statistical analysis were performed using either GraphPad prism 5 or Origin version 8.5. All data are presented as mean±SEM for the given number of experiments. Statistical significance was calculated by a χ^2 test and significance was defined at $P<0.05$.

Results

Super-resolution Scanning Patch Clamp Recording of LTCCs in Ventricular Myocytes

As a first step in the validation of this procedure, we compared results with those obtained (at a very low success rate) by the previously described smart patch-clamp technique, which relied exclusively on the use of a high-resistance pipette (≈100 nm ID, 100 MΩ resistance).[20] In the case described in Figure 4, a pipette with ≈100 nm ID was used to determine the cell topology at high resolution. The tip of the pipette was then clipped to ≈300 nm ID (approximate resistance of 30 MΩ; Figure 2; see Methods) and then repositioned on the cell surface so that the center of the pipette coincided with the center of the selected structure (ie, T-tubule, crest, or groove; diagram in Figure 4A). Figure 4B shows recordings of single LTCC current recorded from the T-tubule using our new procedure. The membrane patch was pulsed to the various voltages indicated in the figure. Figure 4C shows the current traces during consecutive sweeps to the same pulse potential. In this and all other recordings, the seal resistance was >5 GΩ (zero measurable leak current). The stability of the system allowed for recording of ensemble currents, showing time-dependent current inactivation (bottom of Figure 4C). Voltage dependence of activation also was

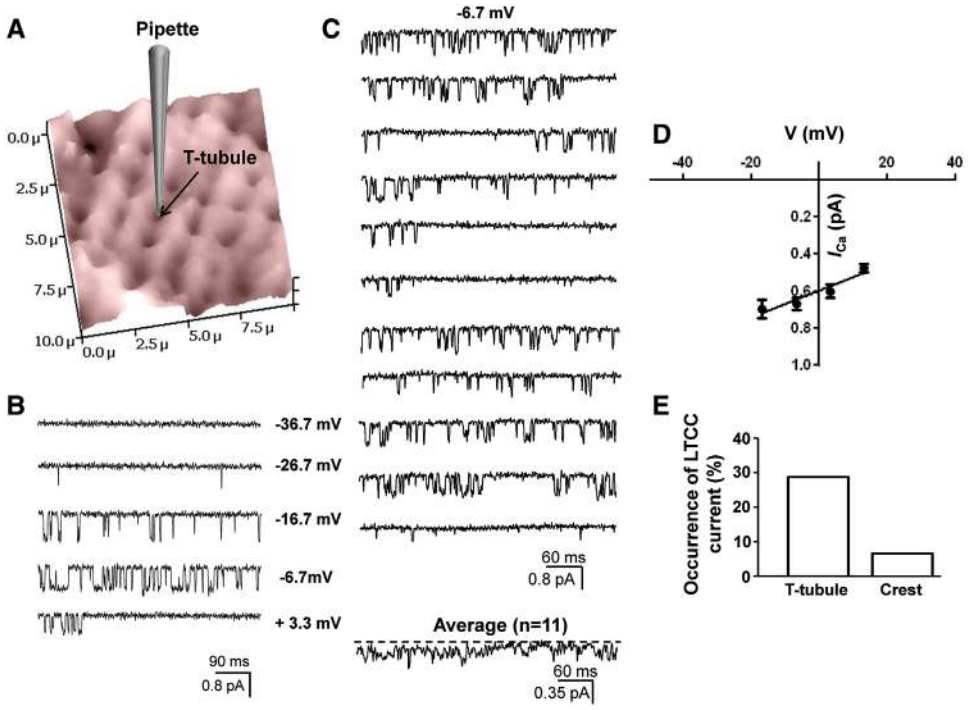

Figure 4. Single L-type calcium channel (LTCC) activity in rat cardiomyocytes. **A**, A 10 µm×10 µm scan of cardiomyocyte revealing topographical structures. The position of the pipette denotes a T-tubule where the pipette was lowered and a gigaseal was obtained. **B**, Representative traces of single LTCC activity recorded from a T-tubule at the given voltages using a pipette of 30 mol/LΩ resistance. **C**, Several sweeps were recorded at −6.7 mV and average of 11 sweeps is shown below. **D**, Current–voltage relationship of single LTCC activity. A voltage dependence was observed in our experiments as expected (n= 5–13 for each data point). **E**, Percent of occurrence of functional LTCCs on the cardiomyocyte sarcolemma. $P<0.02$ when comparing the occurrence of channel activity in patches formed at the T-tubule vs the crest (χ^2 test).

observed in our experiments as expected for voltage-gated LTCCs (Figure 4D). The overall parameters recorded are in agreement with those previously published.[20] The probability of observing LTCC activity in cell-attached mode using this procedure increased from negligible[20] to 28.75% (LTCC activity observed in 23 of 80 patches in T-tubules of cardiomyocytes). Using this new method, we assessed the likelihood of detecting LTCCs in a separate region of the sarcolemma. Of 30 patches formed in the crest region, only 2 showed channel activity (6.6%; $P<0.02$; Figure 4E). Moreover, exposure to isoproterenol caused an increase in channel open probability recorded at the T-tubule, from 0.02 to 0.05, 0.03 to 0.05, and 0.028 to 0.04, respectively, in the 3 experiments attempted. The low occurrence of channels at the crest, their sensitivity to isoproterenol, and their biophysical properties are all consistent with the notion that we selectively recorded from LTCCs, with a spatial resolution in the nanoscale.[21,22] Of note, the probability of recording LTCCs on the surface of neonatal rat ventricular myocytes, which lack T-tubular structures,[23] was 30.8% (LTCC activity observed in 4 of 13 separate recordings; Online Figure IIA and IIB), suggesting that the structural organization of the T-tubule coincides with increased clustering of functional LTCCs at that specific location.

Further increasing the pipette diameter to ≈600 nm (pipette resistance ≈16 MΩ) drastically increased the probability of recording channels (3 of 3 attempts; Figure 5A). Moreover, as shown in Figure 5B, the larger pipette size also increased the likelihood of detecting >1 channel within the area of recording. The process of clipping the pipette tip was highly controlled, and it did not affect the probability of forming a gigaseal on the cardiomyocyte membrane. We observed a similar success rate of gigaohm seal formation (≥5 GΩ) regardless of whether we clipped (70%) or did not clip (68.5%) the pipette tip. Overall, the method described allowed for a dramatic increase in the probability of observing ion channel activity from cell-attached patches formed at a specific location.

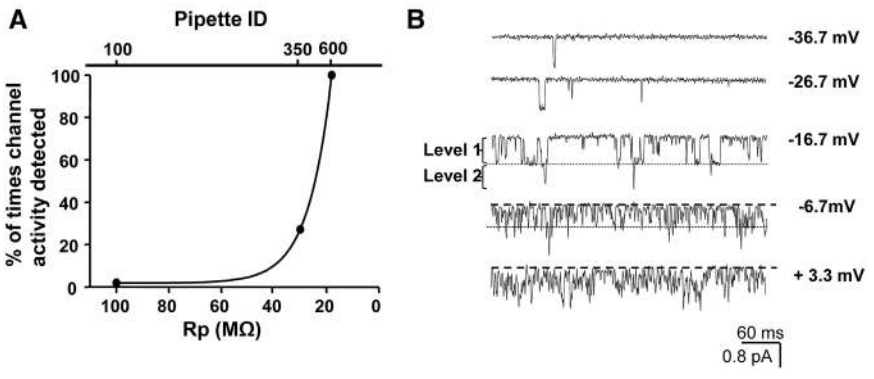

Figure 5. Relationship between pipette resistance and probability of observing single L-type calcium channels (LTCC) activity. **A**, The graph depicts that clipping the pipette tip to 20 mol/LΩ or lower greatly increases the chance of recording single LTCC activity in the T-tubules of cardiomyocytes. Lower *x*-axis is pipette resistance (Rp) and upper *x*-axis denotes estimated pipette internal diameter (ID). **B**, Representative traces of LTCC activity recorded from a T-tubule at the given voltages using a pipette of 16 mol/LΩ resistance. Note that 2 channels could be recorded at the same time. Level 1 and level 2 denote the amplitude of 2 single channels.

Unitary Conductance of Sodium Channels as a Function of Location

Previous studies have shown that the voltage gating properties of cardiac sodium channels and the molecular partners of $Na_V1.5$ proteins are different depending on their location in the cell.[7,9] Here, we used super-resolution scanning patch clamp to directly address the question of whether the single channel unitary conductance of sodium channels varies depending on their spatial location in the cardiomyocyte sarcolemma. Recording conditions (bath and pipette solutions, as well as voltage clamp protocols) were adjusted for recording of tetrodotoxin-dependent channels, as in previous studies.[7] Figure 6 shows individual current traces obtained from sodium channels localized on the area of the T-tubule, as identified by super-resolution scanning patch clamp. Horizontal dotted lines represent unitary current steps. All-points histograms obtained from each trace (data not shown) allowed measurement of step current amplitudes. A compilation of all amplitudes at 1 voltage in the same cell produced a histogram of events (Figure 6B; 124 events at Vm=−70 mV); the same procedure repeated at various voltages yielded a unitary current–voltage relation plot (calculated from 114, 124, 97, and 130 events captured during voltage steps to −80, −70, −60, and −50 mV, respectively); a projection of the line joining the data points over the *x*-axis revealed the reversal potential of the channel (+29 mV) and a unitary slope conductance of 10 pS (Figure 6C). This value is similar to the one previously reported.[24] Using the same approach, we determined that the unitary conductance of channels located in the intercalated disc area is also 10 pS, thus indicating that the differences in current amplitude between the 2 regions, described before,[7] result from differences in the total number of functional channels in each region, rather than variations in unitary conductance properties. Of note, currents were not recorded from patches formed with pipettes filled with a solution containing 30 µmol/L of tetrodotoxin (n=10), further confirming the identity of the channels recorded in the absence of this highly selective blocker. We then proceeded to determine whether channels gathered homogenously in the sarcomere or clustered in confined nanodomains.

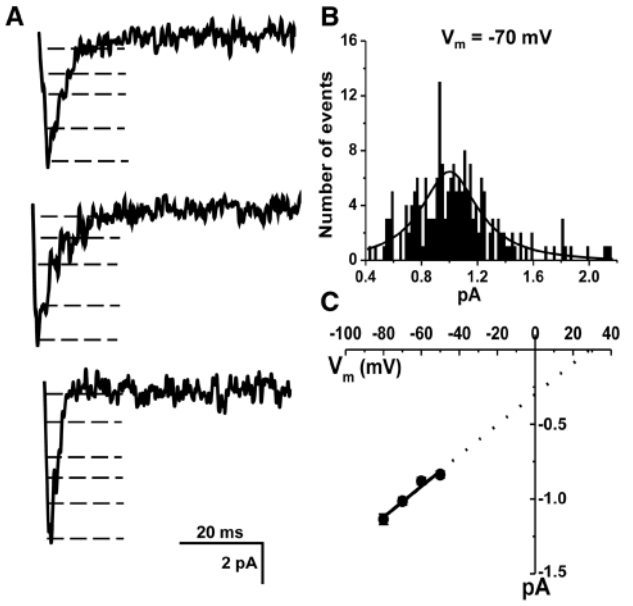

Figure 6. Single sodium channel activity in mouse cardiomyocytes. A, Current traces obtained from a T-tubule of an adult mouse cardiomyocyte using super-resolution scanning patch clamp. Traces have been inverted for consistency with other publications. Voltage steps to −70 mV from a holding potential of −120 mV (polarity referred to the intracellular space). Horizontal dotted lines reflect current steps indicative of unitary events. **B**, Histogram of unitary current amplitude and best-fit Gaussian (red line) corresponding to mean unitary current for that particular family of events. **C**, Cumulative data for unitary current amplitude at various command voltages. Dotted line represents the extrapolation used to calculate the reversal potential and slope unitary conductance of the channels. Each data point corresponds to average of 114, 124, 97, and 130 events captured during voltage steps to −80, −70, −60, and −50 mV, respectively.

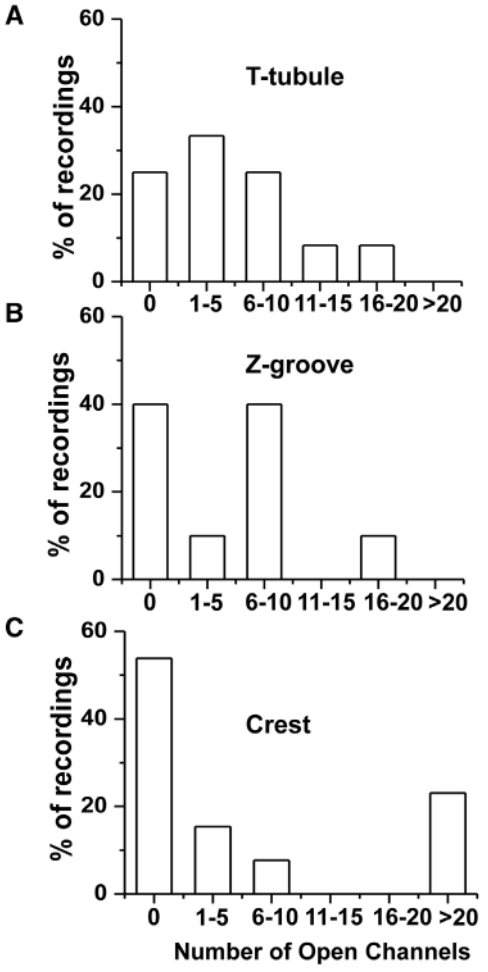

Figure 7. Histograms indicating sodium channel clustering as a function of recording location. Ordinates show percent of recordings (relative to total number of attempts). Abscissae show number of open channels detected. Number of open channels in each recorded patch was estimated from the average peak current amplitude (10 sweeps) during a voltage step to −30 mV from a holding potential of −120 mV, and an estimated unitary conductance of 10 pS (see data in Figure 6). Total number of attempts: 12, 10, and 13 for T-tubule (**A**), Z-groove (**B**), or crest (**C**), respectively. $P<0.02$ when comparing the occurrence of >20 channels in crest vs Z-groove and T-tubules (χ^2 test).

Regional Differences in Sodium Channel Distribution on the Cardiomyocyte Sarcolemma

The technical advancement described allowed us to study, for the first time, the subcellular distribution of functional sodium channels in the adult cardiomyocyte sarcolemma. After scanning the cell surface, pipette ID was increased to ≈500 nm (≈22 MΩ resistance). The SICM topography image allowed us to choose the precise recording location. Results are summarized in Figure 7. Figure 7A through 7C present histograms of the percent of recordings that yielded currents of various magnitudes. The abscissae are expressed as number of open channels calculated based on a unitary conductance of 10 pS (as per data in Figure 6). The number of open channels was estimated from the peak average current recorded in 10 consecutive sweeps. We obtained a total of 12 recordings in which the pipette was placed over the opening of a T-tubule. Three of those recordings showed a complete absence of channels. In the other 9 cases, we recorded an average of 8 channels per patch (Figure 7). The distribution of functional sodium channel population in the Z-groove was bimodal, with recordings showing either absence of current elicited by the voltage clamp step or clusters of 6 to 10 channels (with 2 exceptions). The largest segregation, however, was found in the crest, where we obtained a lower success rate and, yet, a much higher channel density when fast inward currents were recorded. Of 13 patches, only 6 were formed over functional channels (in 7 other patches, the voltage step elicited no time-dependent current). Of those that showed channel activity, 2 contained only 1 or 2 channels and 1 patch showed current amplitude corresponding to 6 channels. Three patches, however, yielded macroscopic currents that were estimated to contain 29, 36, and 47 channels, respectively. These large macroscopic currents were only observed in the recordings from the crest region and reveal a high degree of sodium channel clustering, with up to ≈50 channels occupying confined areas of <0.4 μm^2 (assuming a hemispherical shape of the membrane patch) likely separated by other areas void of activity. The occurrence of >20 channels in the crest compared with Z-groove and T-tubules was statistically significant (P<0.02; Figure 7C). Of note, this segregation was not observed in recordings from neonatal rat ventricular myocytes, in which we observed a more Gaussian distribution of events when recording from the cell surface (Online Figure IIC).

Discussion

Several studies have demonstrated the existence of cell surface microdomains, which are important for compartmentation of cellular signaling.[18,25,26] Ion channels and receptors, which are an integral part of these signaling microdomains, are thus spatially confined. Yet, a method that allows the study of spatial distribution of ion channel proteins together with a characterization of their location-specific function is lacking. Immunofluorescence microscopy is limited by its spatial resolution (≈250–300 nm)[27] and does not allow a functional assessment of the channel. Patch clamp, however, provides data on the functional properties of the channels, but the site of recording is only grossly approximated by standard methods.[7,28] In recent studies, investigators combined SICM with patch clamp to study the activity of ion channels from microdomains in the sarcolemma with a nanoscale resolution.[20,22,29,30] The power of this method, however, was limited by its low throughput, as shown in a previous study[24] in which only 1 sweep of 1 recording of a sodium channel was presented without possibility of quantitation or further characterization of location-specific activity. In the current study, we have validated a new method for studying clustering of ion channels with increased success rate by using a combination of patch clamp and SICM, plus a software modification that allowed for a precisely controlled increase in the pipette tip diameter. As a result, a fine-tipped pipette can be used for characterization of surface topology and, then, a wider pipette can be used for location-specific recording of electrophysiological properties. The larger pipette tip diameter greatly increases the success rate of detecting ion channel activity because of an increase in the membrane area under the patch. The result is the ability to record ion channels from a specific site with nanoscale precision. Because of the similar spatial resolution achieved by super-resolution microscopy,[10] we refer to this new method as super-resolution scanning patch clamp.

To validate the new method, we defined the spatial location of functional LTCCs on the surface of cardiomyocytes. Immunofluorescence microscopy indicates that LTCC proteins are highly concentrated at T-tubules, in close proximity to ryanodine receptors, thus facilitating excitation–contraction coupling.[4] SICM-guided patch clamp had confirmed that, as predicted by immunofluorescence studies, functional LTCCs are found at the T-tubules, unlike ion channels, such as K_{ATP}[30] and maxi-anion channels,[29] which were observed to be uniformly distributed along Z-grooves. A systematic study was prevented by the very low throughput of this method. Here, we used super-resolution scanning patch clamp to increase our success rate of recording functional channels from negligible[20] to 28.75% (Figure 5A). In addition, 70% of attempts yielded a gigaseal, a success rate similar to that in conventional patch clamp. The applicability of this new method is far-reaching. Recent studies have demonstrated that the structure of the cardiomocyte sarcolemma is disturbed in heart failure.[18,31,32] The fate of LTCCs under that condition remains unknown and, yet, intracellular calcium homeostasis is seen as an important target for therapy in that pathological state.[33] The redistribution of ion channel proteins may carry as a consequence their separation from other molecules that are relevant to their regulation (such as β-adrenergic receptors).[21] Furthermore, as channel proteins redistribute through the cell surface, it is important to identify the molecular clusters that remain as active charge carriers. This information, not provided by simple immunofluorescence, may be critical for target-specific pharmacological design.

Similar arguments apply to the study of sodium channels. It is well-established that Nav1.5 in the cardiomyocyte sarcolemma associates with the syntrophin–dystrophin complex.[9] However, the precise location of functional channels remained undefined. Here, we show that along the crests, functional channels are found in well-populated clusters, coexisting with areas void of electric activity. The latter is reminiscent of what has

been described for other Na_V proteins in the nervous system. A case in point are the node of Ranvier and the axon initial segments, where sodium channels are highly clustered, and their distribution is highly dependent on scaffolding proteins that serve as molecular organizing centers.[34] This is the first demonstration depicting that sodium channels not only segregate into 2 different pools (intercalated disc and lateral membranes, as defined by Petitprez et al[9] or cell midsection as referred to by Lin et al[7]) but also cluster into highly confined functional nanodomains. The fate of these domains under various adaptive, developmental, or pathological conditions (eg, Duchenne cardiomyopathy vis-a-vis excitation-contraction coupling and heart failure) remains to be defined. The method described in this article offers a glimpse at the biology of functional ion channels in cardiomyocytes with an unprecedented level of resolution, thereby providing a platform to quantitatively address these important questions.

Acknowledgments

The authors thank Peter O'Gara for isolation of cardiomyocytes.

Sources of Funding

Supported by grants RO1-HL106632 and RO1-GM57691 from the National Institutes of Health (M. Delmar), Leducq Foundation Transatlantic Network (M. Delmar), Wellcome Trust (J. Gorelik), and British Heart Foundation (J. Gorelik), and by the Imperial College London Rector Award (J. Gorelik).

Disclosures

None.

References

1. Balijepalli RC, Foell JD, Hall DD, Hell JW, Kamp TJ. Localization of cardiac L-type $Ca^{(2+)}$ channels to a caveolar macromolecular signaling complex is required for beta(2)-adrenergic regulation. *Proc Natl Acad Sci USA*. 2006;103:7500–7505.
2. Scriven DR, Dan P, Moore ED. Distribution of proteins implicated in excitation-contraction coupling in rat ventricular myocytes. *Biophys J*. 2000;79:2682–2691.
3. Rybin VO, Xu X, Lisanti MP, Steinberg SF. Differential targeting of beta -adrenergic receptor subtypes and adenylyl cyclase to cardiomyocyte caveolae. A mechanism to functionally regulate the cAMP signaling pathway. *J Biol Chem*. 2000;275:41447–41457.
4. Bers DM. Cardiac excitation-contraction coupling. *Nature*. 2002;415:198–205.
5. Bito V, Heinzel FR, Biesmans L, Antoons G, Sipido KR. Crosstalk between L-type Ca^{2+} channels and the sarcoplasmic reticulum: alterations during cardiac remodelling. *Cardiovasc Res*. 2008;77:315–324.
6. Heinzel FR, MacQuaide N, Biesmans L, Sipido K. Dyssynchrony of Ca^{2+} release from the sarcoplasmic reticulum as subcellular mechanism of cardiac contractile dysfunction. *J Mol Cell Cardiol*. 2011;50:390–400.
7. Lin X, Liu N, Lu J, Zhang J, Anumonwo JM, Isom LL, Fishman GI, Delmar M. Subcellular heterogeneity of sodium current properties in adult cardiac ventricular myocytes. *Heart Rhythm*. 2011;8:1923–1930.
8. Sato PY, Coombs W, Lin X, Nekrasova O, Green KJ, Isom LL, Taffet SM, Delmar M. Interactions between ankyrin-G, Plakophilin-2, and Connexin43 at the cardiac intercalated disc. *Circ Res*. 2011;109:193–201.
9. Petitprez S, Zmoos AF, Ogrodnik J, Balse E, Raad N, El-Haou S, Albesa M, Bittihn P, Luther S, Lehnart SE, Hatem SN, Coulombe A, Abriel H. SAP97 and dystrophin macromolecular complexes determine two pools of cardiac sodium channels Nav1.5 in cardiomyocytes. *Circ Res*. 2011;108:294–304.
10. Schermelleh L, Heintzmann R, Leonhardt H. A guide to super-resolution fluorescence microscopy. *J Cell Biol*. 2010;190:165–175.
11. Korchev YE, Milovanovic M, Bashford CL, Bennett DC, Sviderskaya EV, Vodyanoy I, Lab MJ. Specialized scanning ion-conductance microscope for imaging of living cells. *J Microsc*. 1997;188:17–23.
12. Vescovo G, Jones SM, Harding SE, Poole-Wilson PA. Isoproterenol sensitivity of isolated cardiac myocytes from rats with monocrotaline-induced right-sided hypertrophy and heart failure. *J Mol Cell Cardiol*. 1989;21:1047–1061.
13. Korchev YE, Bashford CL, Milovanovic M, Vodyanoy I, Lab MJ. Scanning ion conductance microscopy of living cells. *Biophys J*. 1997;73:653–658.
14. Hansma PK, Drake B, Marti O, Gould SA, Prater CB. The scanning ion-conductance microscope. *Science*. 1989;243:641–643.
15. Shevchuk AI, Frolenkov GI, Sánchez D, James PS, Freedman N, Lab MJ, Jones R, Klenerman D, Korchev YE. Imaging proteins in membranes of living cells by high-resolution scanning ion conductance microscopy. *Angew Chem Int Ed Engl*. 2006;45:2212–2216.
16. Novak P, Li C, Shevchuk AI, Stepanyan R, Caldwell M, Hughes S, Smart TG, Gorelik J, Ostanin VP, Lab MJ, Moss GW, Frolenkov GI, Klenerman D, Korchev YE. Nanoscale live-cell imaging using hopping probe ion conductance microscopy. *Nat Methods*. 2009;6:279–281.
17. Rheinlaender J, Geisse NA, Proksch R, Schäffer TE. Comparison of scanning ion conductance microscopy with atomic force microscopy for cell imaging. *Langmuir*. 2011;27:697–704.
18. Nikolaev VO, Moshkov A, Lyon AR, Miragoli M, Novak P, Paur H, Lohse MJ, Korchev YE, Harding SE, Gorelik J. Beta2-adrenergic receptor redistribution in heart failure changes cAMP compartmentation. *Science*. 2010;327:1653–1657.
19. Ying L, Bruckbauer A, Rothery AM, Korchev YE, Klenerman D. Programmable delivery of DNA through a nanopipet. *Anal Chem*. 2002;74:1380–1385.
20. Gorelik J, Gu Y, Spohr HA, Shevchuk AI, Lab MJ, Harding SE, Edwards CR, Whitaker M, Moss GW, Benton DC, Sánchez D, Darszon A, Vodyanoy I, Klenerman D, Korchev YE. Ion channels in small cells and subcellular structures can be studied with a smart patch-clamp system. *Biophys J*. 2002;83:3296–3303.
21. Chen-Izu Y, Xiao RP, Izu LT, Cheng H, Kuschel M, Spurgeon H, Lakatta EG. G(i)-dependent localization of beta(2)-adrenergic receptor signaling to L-type $Ca^{(2+)}$ channels. *Biophys J*. 2000;79:2547–2556.
22. Gu Y, Gorelik J, Spohr HA, Shevchuk A, Lab MJ, Harding SE, Vodyanoy I, Klenerman D, Korchev YE. High-resolution scanning patch-clamp: new insights into cell function. *FASEB J*. 2002;16:748–750.
23. Haddock PS, Coetzee WA, Cho E, Porter L, Katoh H, Bers DM, Jafri MS, Artman M. Subcellular [Ca2+]i gradients during excitation-contraction coupling in newborn rabbit ventricular myocytes. *Circ Res*. 1999;85:415–427.
24. Duclohier H. Neuronal sodium channels in ventricular heart cells are localized near T-tubules openings. *Biochem Biophys Res Commun*. 2005;334:1135–1140.
25. Agarwal SR, MacDougall DA, Tyser R, Pugh SD, Calaghan SC, Harvey RD. Effects of cholesterol depletion on compartmentalized cAMP responses in adult cardiac myocytes. *J Mol Cell Cardiol*. 2011;50:500–509.
26. Macdougall DA, Agarwal SR, Stopford EA, Chu H, Collins JA, Longster AL, Colyer J, Harvey RD, Calaghan S. Caveolae compartmentalise β2-adrenoceptor signals by curtailing cAMP production and maintaining phosphatase activity in the sarcoplasmic reticulum of the adult ventricular myocyte. *J Mol Cell Cardiol*. 2012;52:388–400.
27. van de Linde S, Loschberger A, Klein T, Heidbreder M, Wolter S, Heilemann M, Sauer M. Direct stochastic optical reconstruction microscopy with standard fluorescent probes. *Nature Protocols*. 2011;6:991–1009.
28. Verkerk AO, van Ginneken AC, van Veen TA, Tan HL. Effects of heart failure on brain-type Na+ channels in rabbit ventricular myocytes. *Europace*. 2007;9:571–577.
29. Dutta AK, Korchev YE, Shevchuk AI, Hayashi S, Okada Y, Sabirov RZ. Spatial distribution of maxi-anion channel on cardiomyocytes detected by smart-patch technique. *Biophys J*. 2008;94:1646–1655.
30. Korchev YE, Negulyaev YA, Edwards CR, Vodyanoy I, Lab MJ. Functional localization of single active ion channels on the surface of a living cell. *Nat Cell Biol*. 2000;2:616–619
31. Horiuchi-Hirose M, Kashihara T, Nakada T, Kurebayashi N, Shimojo H, Shibazaki T, Sheng X, Yano S, Hirose M, Hongo M, Sakurai T, Moriizumi T, Ueda H, Yamada M. Decrease in the density of t-tubular

L-type Ca2+ channel currents in failing ventricular myocytes. *Am J Physiol Heart Circ Physiol*. 2011;300:H978–H988.
32. Lyon AR, MacLeod KT, Zhang Y, Garcia E, Kanda GK, Lab MJ, Korchev YE, Harding SE, Gorelik J. Loss of T-tubules and other changes to surface topography in ventricular myocytes from failing human and rat heart. *Proc Natl Acad Sci USA*. 2009;106:6854–6859.
33. Hasenfuss G, Teerlink JR. Cardiac inotropes: current agents and future directions. *Eur Heart J*. 2011;32:1838–1845.
34. Dzhashiashvili Y, Zhang Y, Galinska J, Lam I, Grumet M, Salzer JL. Nodes of Ranvier and axon initial segments are ankyrin G-dependent domains that assemble by distinct mechanisms. *J Cell Biol*. 2007;177:857–870.

Novelty and Significance

What Is Known?

- Sodium and calcium channels are essential for cardiac excitation and contraction.
- These channel proteins compartmentalize to different cell surface regions. However, their precise locations and location-specific functions remain undefined.
- There is a lack of experimental tools to associate ion channel function with its precise location.

What New Information Does This Article Contribute?

- We describe a novel technique called super-resolution scanning patch clamp that allows us to image live cell topography and then record ion channels at a chosen location with nanometer resolution.
- We show that calcium channels are primarily confined to T-tubules, whereas sodium channels in the cell midsection segregate into clusters of variable density depending on the location.
- The major segregation is found in the crests, where areas void of channel activity separate clusters containing >20 channels.

Our studies show the existence of >1 sodium channel pool in the midsection of the cardiomyocyte. Each of these pools may interact with different molecular partners or may be formed by different sodium channel protein subunits. Moreover, we show a new method with broader application in cardiac cellular electrophysiology.